Kinetics and Column Dynamics for Adsorption of Bulk Liquid Mixtures

S. Sircar and M. B. Rao
Air Products and Chemicals, Inc., Allentown, PA 18195

A framework is developed to describe kinetics and column dynamics of ad(de)sorption from bulk liquid mixtures using surface excess as the variable to quantify the extent of adsorption. It is found that the transient rate of change of surface excess with time from a multicomponent liquid mixture can be expressed in terms of a surface excess linear-driving-force model. A local-equilibrium model can be developed to describe the column dynamics of ad(de)sorption from liquid mixtures. Both self-sharpening and proportionate pattern mass-transfer zones can be formed depending on the shape of the surface-excess isotherm and the selectivity of adsorption. Analysis of column dynamics for liquid mixture adsorption can be carried out analogous to that for adsorption from gas mixtures, when a constant pattern mass-transfer zone is formed. The length of the mass-transfer zone and the composition-time column effluent profile can also be derived analytically for such a case. Experimental kinetics and column dynamics data for ad(de)sorption of ethanol-water mixtures on a large-pore activated carbon are analyzed using these models.

Introduction

Actual amounts adsorbed are not meaningful experimental variables for evaluating adsorption from liquid mixtures except for the special case of adsorption of very selectively adsorbed dilute adsorbates (Sircar et al., 1970). Consequently, thermodynamics, kinetics, and column dynamics for adsorption of bulk liquid mixtures must be formulated in terms of Gibbsian surface-excess variables that can be experimentally measured. Thermodynamics of bulk liquid-phase adsorption is very well developed using surface excess variables (Sircar et al., 1972), and numerous models have been proposed to describe adsorption equilibria for liquid mixtures including the complex case of adsorption of nonideal liquid mixtures having unequal adsorbate sizes on heterogeneous adsorbents (Sircar, 1986). The majority of these models, however, are confined to the study of adsorption from binary liquid mixtures.

The subjects of kinetics and column dynamics for adsorption of liquid mixtures, on the other hand, are not fully developed except for adsorption of dilute adsorbates from a bulk solvent. The process, in that case, can be treated analogous to adsorption of trace adsorbates from a gas because the amounts adsorbed can be approximately estimated. There is a need for describing kinetics and column dynamics for adsorption of bulk liquid mixtures using surface-excess variables because of their practical application in the design of separation processes (Sircar, 1991a,b; Chen and Sircar, 1991). The purpose of this article is to develop a simple mathematical framework in that direction.

The specific surface excess (n_i^e) for adsorption of component i (mol/kg) of a liquid mixture containing N components in contact with a solid adsorbent is given by (Sircar et al., 1972):

$$n_i^e = n_i - x_i \sum_i n_i \quad i = 1,2 \ldots N \tag{1}$$

where n_i is the actual specific amount of component i adsorbed (mol/kg) on the adsorbent in contact with the liquid mixture. x_i is the mole fraction of that component in the bulk liquid mixture. n_i^e is the nonequilibrium transient surface excess of component i when n_i is the transient specific amount adsorbed of that component in contact with a liquid mixture of composition x_i. Equation 1 also defines the equilibrium specific surface excess (n_i^{e*}) of component i in contact with a bulk liquid of composition x_i:

Correspondence concerning this article should be addressed to S. Sircar.

$$n_i^{e*} = n_i^* - x_i \sum_i n_i^* \quad i = 1,2 \ldots N \tag{2}$$

where n_i^* is the specific amount of component i adsorbed at equilibrium.

The constraint ($\Sigma x_i = 1$) implies that:

$$\sum_i n_i^e = \sum_i n_i^{e*} = 0 \tag{3}$$

The summation in Eq. 3 is over all components of the liquid mixture. Equation 3 shows that only $(N-1)$ surface excess variables need to be defined for an N-component system.

The quantities n_i and n_i^* cannot be experimentally measured for adsorption from bulk liquid mixtures, but it can be shown by carrying out the material balance between a bulk liquid phase and a Gibbsian adsorbed phase of a liquid-solid adsorption system (Sircar et al., 1972) that:

$$n_i^e = n_i^o - x_i \sum_i n_i^o \tag{4}$$

where n_i^o is the total specific amount of component i in the adsorption system, which can be measured directly. Thus, n_i^e can be experimentally measured by contacting a known amount (n^o) of a liquid mixture of known composition (x_i^o) with unit amount of an adsorbent and by monitoring the change in the bulk liquid composition (x_i) with time (t) until equilibrium is reached. The kinetics of adsorption for a specific system can be estimated by measuring the rate of change of x_i and n_i^e with time:

$$\frac{dn_i^e}{dt} = -[\Sigma n_i^o] \frac{dx_i}{dt} \tag{5}$$

The equilibrium surface excess adsorption isotherm can be expressed as:

$$n_i^{e*} = n_i^{e*}[x_i] \text{ constant } T \tag{6}$$

Surface Excess Linear-Driving-Force Model for Kinetics of Adsorption from Liquid Mixtures

Consider an N-component, isothermal, liquid-phase adsorption system under transient conditions, where the bulk liquid-phase composition (x_i) is held constant. Equation 1 can be differentiated with respect to time to describe the rate of change of n_i^e with time for the system as:

$$\frac{dn_i^e}{dt} = \frac{dn_i}{dt} - x_i \sum_i \frac{dn_i}{dt} \tag{7}$$

where n_i, in this case, is the specific amount of component i adsorbed at time t.

We assume that the monolayer-pore filling (MPF) model of adsorption applies (Sircar, 1986). This model has been extensively used to describe adsorption equilibrium for multicomponent liquid-phase systems. It implies that adsorption from the liquid phase is restricted to a monolayer on a nonporous adsorbent or that the total pore volume of a porous adsorbent defines the adsorption space. Since the characteristics of adsorption from liquid phase require that a monolayer is always formed or the pores remain always filled with the liquid mixture, the MPF model yields:

$$\sum_i \frac{n_i(t)}{m_i} = 1 \tag{8}$$

$$\sum_i \frac{n_i^*}{m_i} = 1 \tag{9}$$

where n_i^* is the specific amount of component i adsorbed at equilibrium with a bulk-phase composition of x_i, and m_i is the monolayer adsorption capacity (mol/m^2) or the specific saturation pore-filling capacity (mol/kg) of pure-liquid adsorbate i on the adsorbent.

We also assume that the well-known linear-driving-force (LDF) model (Yang, 1987) for adsorption describes the transient rate of adsorption of component i for the liquid-solid system.

$$\frac{dn_i(t)}{dt} = k_i[n_i^*(x_i) - n_i(t)] \quad i = 1,2 \ldots N \tag{10}$$

where n_i^* and n_i^{e*} are related by Eq. 2, and k_i is the lumped adsorptive mass-transfer coefficient (inverse seconds) for adsorption of component i. Equation 10 has been very successfully applied to describe kinetics of multicomponent gas adsorption in practical systems (Yang, 1987).

For a given x_i [$\Sigma x_i = 1$] and a set of k_i and m_i ($i = 1,2 \ldots N$) values, there are $(5N-3)$ unknown parameters for the kinetic system in view of Eq. 3. They are $n_i(t)$, n_i^*, $n_i^e(t)$, n_i^{e*}, and $(dn_i^e/\mathrm{d}t)$. Equations 1-3 and 7-10 provide $(5N-3)$ independent equations relating them. Thus, $(dn_i^e/\mathrm{d}t)$ can be expressed in terms of n_i^{e*} and n_i^e. All of these three variables can be experimentally measured. For example, the kinetics of adsorption of a three-component liquid system ($N=3$) can be described by:

$$\frac{dn_1^e}{dt} = k_1[n_1^{e*} - n_1^e] + \frac{(k_1 - k_2)}{\Psi} x_1\beta_1(1-\beta_2)(n_2^{e*} - n_2^e) + \frac{(k_1 - k_2)}{\Psi}(1-\beta_1)(1-\beta_2)[x_1x_3(n_2^{e*} - n_2^e) - x_1x_2(n_3^{e*} - n_3^e)] \tag{11}$$

$$\frac{dn_2^e}{dt} = k_2[n_2^{e*} - n_2^e] - \frac{(k_1 - k_2)}{\Psi} x_2\beta_2(1-\beta_1)(n_1^{e*} - n_1^e) - \frac{(k_1 - k_2)}{\Psi}(1-\beta_1)(1-\beta_2)[x_2x_3(n_1^{e*} - n_1^e) - x_1x_2(n_3^{e*} - n_3^e)] \tag{12}$$

where $\Psi = [1-(1-\beta_1)x_1 - (1-\beta_2)x_2]$, $\beta_1 = (m_3/m_1)$ and $\beta_2 = (m_3/m_2)$.

Only Eqs. 11 and 12 are needed to describe the system completely because of the constraint given by Eq. 3. They show two very interesting features: (a) the rate of change of surface excess of component i during the transient process depends

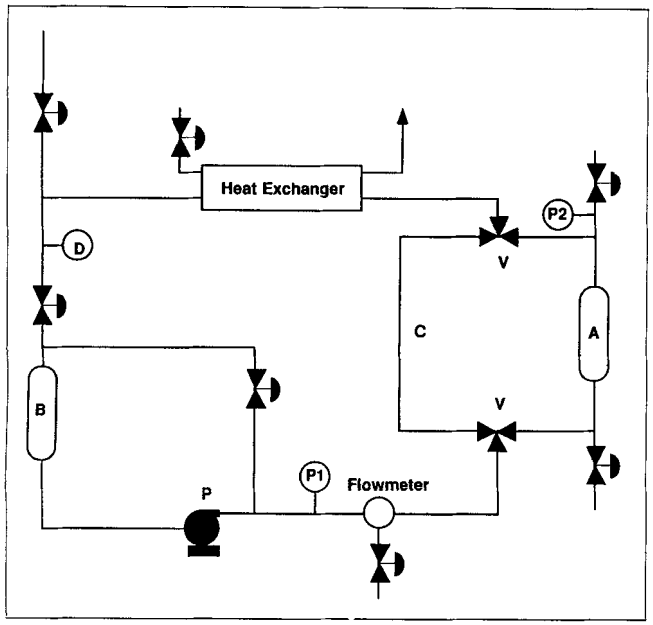

Figure 1. Differential kinetic test apparatus.

not only on the difference between the equilibrium surface excess and the transient surface excess of that component at time t, but also on such differences for other components present in the system; (b) only two of the mass-transfer coefficients are needed to describe the transient three-component system, because k_1, k_2, and k_3 must be related to each other to satisfy Eqs. 3, 8 and 9.

For the special case, where the adsorbates have equal sizes [m_i = constant, $\beta_i = 1$], Eqs. 11 and 12 reduce to:

$$\frac{dn_i^e}{dt} = k_i[n_i^{e*} - n_i^e] \quad i = 1,2\ldots(N-1) \tag{13}$$

Equation 13 shows that, in this case, the rate of change of surface excess of component i depends linearly on the surface excess driving force, $(n_i^{e*} - n_i^e)$, for adsorption of that component. This behavior is identical to the LDF model for gas adsorption using the difference between the equilibrium and actual amounts adsorbed as the driving force for mass transfer (Eq. 10).

For transient adsorption from a binary solution ($i = 1,2$), it can be shown that Eq. 13 describes the rate of change of surface excess of component 1 irrespective of the values of m_1 and m_2. Thus, the present surface excess LDF model (Eq. 13) is very general in describing transient surface excess for a binary liquid system. It can also be shown that $k_1 = k_2$ for such a system.

It should be emphasized that Eqs. 11-13 are exact for the MPF model only. They, however, illustrate several interesting features of multicomponent, liquid-phase mass-transfer kinetics, which are not obvious.

Differential Kinetic Test

The surface-excess LDF model developed above can be used to estimate the mass-transfer coefficients (k_i) for the liquid adsorption system. However, a differential kinetic test is required to satisfy the constraint of constant x_i during the transient process. This can be achieved by using a closed-loop circulating apparatus as depicted in Figure 1. It consists of an adsorption cell (A) containing the adsorbent, a liquid holder (B), a by-pass line (C), a liquid circulating pump (P), two three-way valves (V), and a composition monitoring device (D). The volumes of the adsorption cell with the adsorbent in place, the liquid holder, the by-pass line and the entire system must be calibrated beforehand. The experiment consists of filling the adsorbent cell with a predetermined quantity of a pure liquid or a mixture of known composition and the rest of the system (including the bypass line) with another predetermined quantity of pure liquid or a mixture of known composition.

The pump can be used to circulate the liquid in the closed-loop system through the bypass line, and then the flow can be switched through the adsorbent cell by closing off bypass line with appropriate valves at time $t = 0$. The change in bulk-phase composition of the liquid mixture (x_i) in the system can then be monitored as a function of time (t) using D until equilibrium ($x_i = x_i^*$) is reached (no change in x_i with t). By controlling the amount of adsorbent in the cell and the size of the liquid holder and pipelines, it is fairly easy to achieve a differential test where the composition of the liquid phase does not change significantly (< 5% change in x_i) between the initial mixed composition (x_i^o) and the equilibrium composition (x_i^*) in the system. x_i^o can be calculated by knowing the quantities and compositions of liquid mixtures in different parts of the apparatus at the start of the experiment. The data analysis for a binary isothermal system can be done as follows.

The rate of change of surface excess during the differential test can be calculated by (Eq. 5):

$$\frac{dn_1^e}{dt} = -n^o \frac{dx_1}{dt} \tag{14}$$

where n^o is total moles of liquid per unit amount of the adsorbent in the system volume minus the bypass loop. The surface-excess LDF model gives the instantaneous rate of change of that variable:

$$\frac{dn_1^e}{dt} = k_1[n_1^{e*}(x_1) - n_1^e(t)] \tag{15}$$

where $n_1^{e*}(x_1)$ is the equilibrium surface excess of component 1 at composition x_1. Since the experiment is conducted with a small change in bulk liquid-phase composition ($x_1^o \sim x_1^*$), one can write:

$$n_1^{e*}(x_1) = n_1^{e*}(x_1^*) + b(x_1 - x_1^*) \tag{16}$$

where b is the slope of the surface excess isotherm at x_1^*, and $n_1^e(t)$ is related to $n_1^{e*}(x_1^*)$ during the experiment by:

$$n_1^e = n_1^{e*} + n^o(x_1^* - x_1) \tag{17}$$

Equations 14-17 can be combined to get:

$$\frac{dx_1}{(x_1 - x_1^*)} = -k_1 \frac{(n^o + b)}{n^o} dt \tag{18}$$

which can be integrated to obtain:

$$\ln|(x_1-x_1^*)| = -k_1\frac{(n^o+b)}{n^o}t+\ln(x_1^o-x_1^*) \qquad (19)$$

Thus, a plot of $\ln|(x_1-x_1^*)|$ against time (t) for the differential test should yield a straight line with a slope of $-k_1[(n^o+b)/n^o]$. Hence, k_1 can be calculated knowing b from an independently measured surface excess isotherm for the system of interest. Typically, $n^o \gg b$, and the slope of the above described plot is approximately equal to $-k_1$.

In practice, the measured bulk-phase composition of the liquid mixture will initially ($t=0$) be equal to the liquid composition in the holder (B) and by-pass line (C). After a short mixing time, the measured composition will become equal to the instantaneous composition in contact with the adsorbent in the cell (A). Therefore, only the $x_1(t)$ data acquired after the appropriate mixing time should be used in Eq. 19 for the calculation of k_1.

The procedure can be repeated to obtain k_1 as a function of x_1^*, both for adsorption and desorption processes by appropriately choosing the initial liquid compositions in the adsorption cell and the rest of the system. The effect of external film resistance can also be evaluated in this apparatus by varying the liquid circulating rate. A previous publication (Rao et al., 1991) provides some actual experimental data measured in our laboratory and their analysis using this procedure.

Bulk Liquid-Phase Column Dynamics

The key process steps for separating bulk liquid mixtures by selective adsorption in a fixed adsorption column consist of displacing a pure liquid or a mixture from a column by another pure liquid or mixture. Adsorption or desorption takes place when a more strongly adsorbed species displaces a less strongly adsorbed species from the column or vice versa. A series of separation schemes, called concentration swing adsorption processes, have been recently developed using various combinations of these displacement steps (Sircar, 1991a,b; Chen and Sircar, 1991). The isothermal column dynamics for these steps can be evaluated for a binary system by solving simultaneously the following two mass-conservation equations:

$$\rho_b\left(\frac{\partial\bar{n}_1}{\partial t}\right)_z = -\left\{\frac{\partial[Qx_1]}{\partial z}\right\}_t \qquad (20)$$

$$\rho_b\left(\frac{\partial\bar{n}}{\partial t}\right)_z = -\left(\frac{\partial Q}{\partial z}\right)_t \qquad (21)$$

These equations are derived by assuming that there is no axial dispersion or radial distribution of composition within the column. $\bar{n}_i$ and $\bar{n}$ are the total specific amount of component i (mol/kg) and the total specific amount of all components (mol/kg), respectively, in the column at a distance z from the feed end ($z=0$) at time t. The total amounts in the column include materials in the intra- and interparticle void spaces, as well as the adsorbed phase. Q is the total molar flow rate per unit cross-sectional area of the empty column (mol/m^2·s) through the column at z and t. x_i is the bulk liquid-phase mole fraction of component i at z and t. ρ_b is the bulk density of the adsorbent. An overall mass balance between the adsorbed and bulk liquid phases at any section of the column gives:

$$\bar{n}_1 = n_1^e + x_1\bar{n} \qquad (22)$$

where n_i^e is the surface excess of component i in the column (mol/kg) at z and t. Equations 20-22 can be combined to get:

$$-Q\left(\frac{\partial x_1}{\partial z}\right)_t = \rho_b\left(\frac{\partial n_1^e}{\partial t}\right)_z + \rho_b\bar{n}\left(\frac{\partial x_1}{\partial t}\right)_z \qquad (23)$$

Equations 21 and 23 describe the column dynamics in terms of x_i, n_i^e, $\bar{n}$ and Q, which are functions of z and t. The local rate of change of n_i^e at any z and t can be expressed by using the LDF model (Eq. 13). The local $n_i^{e*}(x_i)$ can be obtained from independent isotherm measurement. Thus, there are four unknowns for a binary system ($\bar{n}_1$, $\bar{n}$, x_1, and Q), and three independent equations (Eqs. 13, 21 and 23) relating them. It is not possible to solve them uniquely without measuring independently the breakthrough curve (x_1 vs. t at any z) or the Q vs. t profile at the column exit ($z=L$) during the displacement tests.

On the other hand, the quantity $\bar{n}$ as a function of x_i can be measured under equilibrium conditions ($\bar{n}=\bar{n}^*$). It can be done by filling a clean adsorbent column with a liquid mixture of composition x_i and pouring the liquid mixture through the column until the effluent concentration equals x_i. $\bar{n}^*$ can then be calculated by accounting for the amount of liquid introduced and removed from the column. It should be emphasized that $\bar{n}^*$ depends on column shape and its packing conditions. It may be useful to use $\bar{n}^*(x_1)$, instead of $\bar{n}(x_1)$, as the first approximation for solving Eqs. 13, 21 and 23 to estimate the column dynamics.

Local Equilibrium Conditions

If we assume that instantaneous local equilibrium ($k_1 \to \infty$) is established within the column [$n_i^e = n_i^{e*}(x_1)$, $\bar{n}=\bar{n}^*$], then the method of characteristics developed for gas-phase adsorption can be implemented to study column dynamics for liquid adsorption. We define a velocity (β) for the bulk liquid element of composition x_1 traveling through the column:

$$\beta(x_1) = \left(\frac{\partial z}{\partial t}\right)_{x_1} = -\left(\frac{\partial x_1}{\partial t}\right)_z \Big/ \left(\frac{\partial x_1}{\partial z}\right)_t \qquad (24)$$

Equations 20-22 and 24 can be solved immediately for the case of a binary system, where a feed liquid of composition x_1^F is displacing an initial saturating liquid of composition x_1^S in the column to obtain:

$$\beta(x_1) = \frac{Q^F \exp\left[\int_{x_1^F}^{x_1}\frac{d\bar{n}^*}{\bar{n}^*+b}\right]}{\rho_b[\bar{n}^*(x_1)+b(x_1)]} \qquad (25)$$

where Q^F is the flow rate of the feed liquid into the column at $z=0$, and b is the slope of the equilibrium surface excess isotherm at x_1. It can also be shown that:

$$\frac{Q(x_1)}{Q^F} = \exp\left[\int_{x_1^F}^{x_1} \frac{d\bar{n}}{\bar{n}^* + b}\right] \tag{26}$$

where Q is the flow rate of fluid element with mole fraction of x_1 for component 1. The quantities $\beta(x_1)$, $Q(x_1)$ and $Q^s(x_1^s)$ can be calculated for a given x_1^F, x_1^S, and Q^F. The time taken $[t(x_1)]$ for a fluid element of composition x_1 to reach a distance z in column is given by:

$$t(x_1) = z/\beta(x_1) \tag{27}$$

Self-sharpening front

If the component 1 of the binary liquid mixture is more selectively adsorbed than component 2 and $x_1^F > x_1^S$, then the column is in adsorption mode of operation and x_1 varies from x_1^S to x_1^F within the column. If $\beta(x_1)$ increases with increasing x_1, then an unstable mass-transfer zone is formed within the column that collapses to form a vertical breakthrough curve. This is known as a self-sharpening front under local equilibrium conditions. This is a common occurrence for gas adsorption (Yang, 1987). We analyzed the situation for adsorption of an ideal binary liquid mixture of equal adsorbate sizes ($m_1 = m_2 = m$) on a homogeneous adsorbent. The equilibrium surface-excess isotherm by the MPF model for this case (Sircar et al., 1972) is:

$$n_1^{e*} = \frac{mx_1(1-x_1)(S-1)}{(S-1)x_1 + 1} \tag{28}$$

where $S[= n_1^* x_2 / n_2^* x_1]$ is the constant selectivity of adsorption for component 1 over component 2.

Equations 25 and 28 can be combined to get:

$$\beta(x_1) = \frac{Q^F}{\rho_b \bar{n}^*} \frac{[1+c][(S-1)x_1 + 1]^2}{[\{(S-1)x_1 + 1\}^2 + cS]} \tag{29}$$

$$\frac{d\beta}{dx_1} = \frac{2Q^F}{\rho_b \bar{n}^*} \frac{c(1+c)S(S-1)[(S-1)x_1 + 1]}{[\{(S-1)x_1 + 1\}^2 + cS]^2} \tag{30}$$

where $c = (m/\bar{n}^*)/[1 - (m/\bar{n}^*)]$. $\bar{n}^*$, in this case, is independent of x_1.

Equation 30 shows that $d\beta/dx_1 > 0$ at all values of x_1 when $S > 1$. In other words, the shape of the surface-excess isotherm given by Eq. 28 provides a driving force for formation of a self-sharpening mass-transfer zone. A U-shaped isotherm is given by Eq. 28, which is quite common for binary liquid-phase adsorption. In fact, Eq. 28 can empirically describe many surface-excess isotherms even when the liquid forms a nonideal mixture, $m_1 \neq m_2$ and the adsorbent is heterogeneous. Thus, in the adsorption mode of operation, a U-shaped isotherm self-sharpens the mass-transfer zone.

Furthermore, it can be shown from Eqs. 29 and 30 that the larger the values of S and c, the larger is the ratio $\beta(x_1^F)/\beta(x_1^S)$, which increases the driving force for self-sharpening of the zone. c can be increased by increasing $(m/\bar{n}^*)$, which is the ratio of the pore-filling capacity to the column saturation capacity of the adsorbates for the present case.

In the absence of adsorptive mass-transfer resistances, the mass-transfer zone in a self-sharpening situation will be a vertical line within the column where the concentration of component 1 varies from x_1^F to x_1^S. The specific amounts (mol/kg) of feed liquid mixture (F^A) and column effluent (E^A) during the displacement process in this case are given by:

$$F^A = \lambda + \bar{n}^*(x_1^F) \tag{31}$$

$$E^A = \lambda + \bar{n}^*(x_1^S) \tag{32}$$

$$\lambda = \frac{[n_1^{e*}(x_1^F) - n_1^{e*}(x_1^S)]}{x_1^F - x_1^S} \tag{33}$$

Proportionate Pattern Front

Equation 30 shows that $d\beta/dx_1 < 0$ at all values of x_1 when $S < 1$. In this case, there is no driving force for self-sharpening, and the mass-transfer zone elongates as it moves through the column. This is known as proportionate pattern zone. It happens for adsorption of liquid mixtures when component 1 is less selectively adsorbed than component 2 ($S < 1$) and $x_1^F > x_1^S$. The column then operates in the desorption mode.

A proportionate pattern front is also formed when $S > 1$ and $d\beta/dx_1 > 0$, and when $x_1^F < x_1^S$. This is actually a desorption case since the feed is richer in the less strongly adsorbed component than the initial saturating liquid in the column.

The concentration profile within a column for a proportionate pattern zone under local equilibrium conditions can be traced by using Eqs. 25-27. They can also be used to calculate the column effluent ($z = L$) composition and flow rate profiles. The effluent, in this case, consists of a liquid mixture of composition x_1^S until the specific amount (mol/kg) of effluent (E_1) is:

$$E_1 = b(x_1^S) + \bar{n}^*(x_1^S) \tag{34}$$

Then, an effluent of varying composition from x_1^S to x_1^F exits from the column until the column is saturated with the feed liquid mixture. The total specific quantity of the second effluent $[E_2(x_1)]$, when the effluent composition is x_1, is given by:

$$E_2(x_1) = b(x_1) - b(x_1^S) \tag{35}$$

and the total specific quantity of component 1 in $E_2(x_1)$ is given by:

$$E_2^1(x_1) = [x_1 b(x_1) - n_1^{e*}(x_1)] - [x_1^S b(x_1^S) - n_1^{e*}(x_1^S)] \tag{36}$$

The total specific quantity of feed liquid (F^D) of composition x_1^F introduced into the column at complete breakthrough ($x_1 = x_1^F$) is:

$$F^D = b(x_1^F) + \bar{n}^*(x_1^F) \tag{37}$$

The actual desorption effluent profile from a column will be compared against the local equilibrium model profile later in this article.

Constant-Pattern Mass-Transfer Zone

When dispersive forces such as axial dispersion or adsorptive mass-transfer resistances are present in the column but the shape of the surface excess isotherm favors self-sharpening of the mass transfer zone, a balance between these two forces may occur, creating a constant-pattern mass-transfer zone. This is frequently observed for gas-phase adsorption (Yang, 1987). For a constant-pattern system, liquid elements of all compositions travel through the column with the same constant velocity ($\bar{\beta}$). The section of the column ahead of the mass-transfer zone remains equilibrated with the composition x_1^S and the liquid flow rate in that section is Q^S. The section of the column behind the mass-transfer zone remains equilibrated with the composition x_1^F, and the liquid flow rate in that section is Q^F. The composition and flow rates change from x_1^S to x_1^F and from Q^S to Q^F, respectively, within the zone. By replacing $\beta(x_1)$ in Eq. 24 by $\bar{\beta}$, and using Eqs. 20 and 21, we can show that for constant pattern zone:

$$\frac{Q(x_1)}{\bar{\beta}} - \rho_b \bar{n}(x_1) = \frac{Q^F}{\bar{\beta}} - \rho_b \bar{n}^*(x_1^F) = \frac{Q^S}{\bar{\beta}} - \rho_b \bar{n}^*(x_1^S) \tag{38}$$

$$\frac{x_1 Q(x_1)}{\bar{\beta}} - \rho_b \bar{n}_1(x_1) = \frac{x_1^F Q^F}{\bar{\beta}} - \rho_b \bar{n}_1^*(x_1^F) = \frac{x_1^S Q^S}{\bar{\beta}} - \rho_b \bar{n}_1^*(x_1^S) \tag{39}$$

Equations 38 and 39 can be solved together to get:

$$\bar{\beta} = \frac{Q^F}{\rho_b[\lambda + \bar{n}^*(x_1^F)]} \tag{40}$$

$$\frac{Q^S}{Q^F} = \frac{\lambda + \bar{n}^*(x_1^S)}{\lambda + \bar{n}^*(x_1^F)} \tag{41}$$

$$\frac{Q(x_1)}{Q^F} = \frac{\lambda + \bar{n}(x_1)}{\lambda + \bar{n}^*(x_1^F)} \tag{42}$$

$$\left[\frac{n_1^e(x_1) - n_1^{e*}(x_1^F)}{x_1 - x_1^F}\right] = \left[\frac{n_1^{e*}(x_1^F) - n_1^{e*}(x_1^S)}{x_1^F - x_1^S}\right] = \lambda \tag{43}$$

Equation 43 is a key relationship. It provides an analytical expression giving $n_1^e(x_1)$ as a function of x_1 within the constant pattern transfer zone. Equation 42 provides the relationship between Q and $\bar{n}$ for a given x_1 within the zone, but it cannot be effectively used because Q or $\bar{n}$ are not known as functions of x_1. However, the $x_1 - t$ profile within the column at a given z or at the column exit ($z = L$) can be calculated. Only the $Q(t)$ profile cannot be estimated. These are unique characteristics of column dynamics for adsorption of liquid mixtures in packed beds. We can analyze the key practical features of adsorption column dynamics using experimental surface excess data without the knowledge of actual amounts adsorbed.

Assuming that the rate of change of n_1^e within the constant-pattern mass-transfer zone is given by the surface excess LDF model for the binary mixture, Eqs. 13 and 43 can be combined and integrated to get:

$$t(\theta) - t_m = +\frac{1}{k_1}\int_{0.5}^{\theta} \frac{d\theta}{(\theta^* - \theta)} \tag{44}$$

where

$$\theta^* = \left[\frac{n_1^{e*}(x_1) - n_1^e(x_1^S)}{n_1^{e*}(x_1^F) - n_1^{e*}(x_1^S)}\right],$$

$$\theta = \left[\frac{x_1 - x_1^S}{x_1^F - x_1^S}\right],$$

$t(\theta)$ is the time required for liquid element of composition x_1 to reach a distance z in the column, t_m is the time required by the first moment of the mass-transfer zone defined by composition [$x_1 = (x_1^F + x_1^S)/2$ or $\theta = 0.5$] to reach z. t_m is given by $z/\bar{\beta}$. For a given z, Q^F, x_1^F and x_1^S, Eq. 40 can be used to calculate $\bar{\beta}$ and t_m, and then Eq. 44 can be used to calculate the $x_1 - t$ profile using the surface excess isotherm, $n_1^{e*}(x_1)$. Alternatively, the length of the mass-transfer zone, L_M, between two preset values of x_1 (or θ) can be calculated using Eqs. 40 and 44 by:

$$L_M = \bar{\beta}(t_2 - t_1) \tag{45}$$

The integration of Eq. 44, in this case, should be carried between the two preset values of θ (θ_1 and θ_2 corresponding to times t_1 and t_2). L_M is a key variable for the process design. The objective is to reduce the value of L_M so that the adsorber efficiency is maximum. $L_M = 0$ corresponds to the local equilibrium case, which is the most desirable operating condition for the adsorber.

For the simple case, where the adsorption step consists of displacing a pure-liquid component 2 ($x_1^S = 0$) in the column by a binary feed mixture of composition x_1^F, and where the surface excess isotherm is given by Eq. 28, it can be shown that:

$$L_M = \left[\frac{Q^F}{\rho_b \bar{n}^*}\right]\left[\frac{1}{k_1}\right]\left[\frac{(1+c)(1-x_1^F)}{Sx_1^F}\right] \times \left[\frac{\{(S-1)x_1^F + 2\}\{(S-1)x_1^F + 1\}}{\{(S-1)x_1^F + 1\} + cS}\right] \ln\left(\frac{1-\phi}{\phi}\right) \tag{46}$$

where ϕ and $(1-\phi)$ define the values of θ_1 and θ_2 at the two bounds of the constant-pattern mass-transfer zone of length L_M.

The above analysis of the constant-pattern mass-transfer zone for liquid-phase adsorption is analogous to that for gas-phase adsorption (Sircar and Kumar, 1983).

Equation 46 shows the obvious results that L_M decreases with decreasing Q^F and increasing k_1 including the case of local equilibrium ($L_M \to 0$ as $k_1 \to \infty$). It also shows that L_M decreases with increasing S, x_1^F, c, and $\bar{n}^*$ for a given ϕ. These results may not be intuitive.

The other important design variable is the feed-handling capacity of the adsorber. For the present case ($x_1^S = 0$), a column of length L will start breaking through component 1 in the

column effluent when the first moment of the mass-transfer zone reaches the distance $(L-0.5\,L_M)$ from the feed end. The time (t_b) required for that to happen is:

$$t_b = \frac{(L-0.5\,L_M)}{\bar{\beta}} \tag{47}$$

Consequently, for a given L_M and Q^F, t_b will be maximum (the largest feed handling capacity of the column before breakthrough of component 1) when $\bar{\beta}$ is minimum. Equations 28, 40 and 43 can be combined to get:

$$\bar{\beta} = \frac{Q^F}{(\rho_b \bar{n}^*)} \frac{(1+c)[(S-1)x_1^F+1]}{[\{(S-1)x_1^F+1\}+cS]} \tag{48}$$

Equation 48 shows that $\bar{\beta}$ decreases when S, c, and $\bar{n}^*$ increases, and x_1^F decreases.

Thus, the column efficiency for the adsorption process is increased when the feed flow rate is low, the mass-transfer coefficient is high, the selectivity of adsorption is high, and the pore-filling capacity of the adsorbates and its ratio with the column saturation capacity are high. Higher composition of component 1 in the feed liquid mixture decreases the column feed-handling capacity, but it also reduces the length of the mass-transfer zone.

The effect of these variables on the desorption process can be estimated by using the local equilibrium model of desorption developed earlier. We consider the case where the column is initially saturated with the more selectively adsorbed pure component 1 and the displacement fluid is pure component 2. Then by using Eqs. 28 and 34–37, one gets for complete desorption $[x_1^S = 1.0,\ x_1^F = 0]$:

$$E_1 = [(\bar{n}^*)(S-c)]/[S(1+c)] \tag{49}$$

$$E_2 = [(\bar{n}^*)c(S^2-1)]/[S(1+c)] \tag{50}$$

$$\hat{x}_1 = 1/(S+1) \tag{51}$$

$$F^D = (\bar{n}^*)(1+cS)/(1+c) \tag{52}$$

where $\hat{x}_1$ is the average composition of component 1 in the second part of the effluent where a mixture of both components exits the column.

The design objectives for efficient column desorption are to maximize E_1 which has a composition of x_1^S, minimize E_2 and F^D, and maximize $\hat{x}_1$. This will maximize the amount of effluent obtained as pure component 1 and minimize the quantity of the desorbent liquid. It will also minimize the quantity of mixed liquid effluent and maximize the composition of component 1 in the mixed liquid.

Equations 49–52 show that E_1 is increased by increasing S and $\bar{n}^*$ although the effect of changing S on E_1 is relatively small. E_1 increases as c decreases. On the other hand, E_2 and F^D decrease when $\bar{n}^*$, S and c decrease. Furthermore, $\hat{x}_1$ increases as S decreases.

Thus, the desorption process is helped by lower $\bar{n}^*$, c, and S, which is exactly opposite to the behavior of the adsorption process. Consequently, the operation of cyclic liquid-phase separation processes consisting of adsorption and desorption steps (Sircar, 1991a,b; Chen and Sircar, 1991) must be optimized by appropriate selection of the adsorption and column properties.

The simple models of kinetics and column dynamics for isothermal ad(de)sorption of bulk liquid mixtures, described earlier, demonstrate that they can be formulated and evaluated in terms of pertinent surface excess variables and there is no need to revert to actual amounts adsorbed as design variables through some model. The key characteristics of the kinetics and column dynamics for ad(de)sorption of liquid mixtures in terms of surface-excess variables, however, have a strong parallel with those for ad(de)sorption of gas mixtures using actual amounts adsorbed as process variables.

Experimental Evaluation of Kinetics and Column Dynamics for Adsorption of Liquid Mixtures

We measured the kinetics and column dynamics for ad(de)sorption of ethanol-water mixtures on a large-pore activated carbon (CAL) produced by Calgon Corporation (Calgon, 1983). The carbon had a total pore volume of 0.94 cm^3/g and a bulk density of 0.44 g/cm^3. About 75% of all pores had diameters greater than 2 nm. The adsorbent particles were 430 μm in diameter. The ethanol (1) + water (2) mixture was highly nonideal with activity coefficients at infinite dilution of 4.25 and 2.56 at 25°C for alcohol and water, respectively (Gmehling et al., 1981). The molar volumes of alcohol and water at 25°C are 59.0 and 18.0 cm^3/mol, respectively, indicating that the adsorbate sizes differ significantly. A gas chromatograph was used to analyze the liquid mixtures.

Adsorption equilibria

The surface-excess isotherm for ethanol-water mixture was measured on the CAL carbon using the conventional technique (Sircar et al., 1972). Figure 2 shows the experimental (circles) isotherm. The U shape of the isotherm shows that ethanol is selectively adsorbed over water at all compositions. The high slope of the isotherm at $x_1 \to 0$ indicates that the selectivity of adsorption for ethanol is very high (Sircar, 1986). The dashed line in Figure 2 shows the best fit of the data by Eq. 28. It may be seen that Eq. 28 describes the data qualitatively even

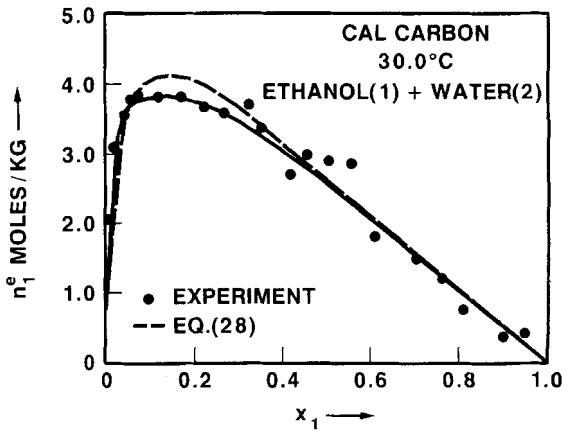

Figure 2. Surface-excess isotherm for adsorption of ethanol (1) + water (2) mixtures on Calgon CAL carbon at 30°C.

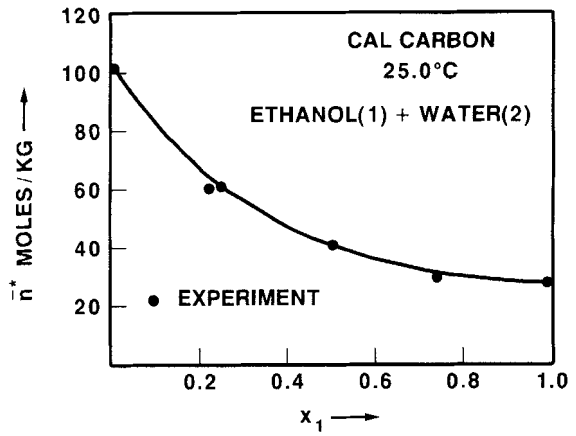

Figure 3. Specific saturation capacities of a packed CAL carbon column for ethanol (1) + water (2) mixtures of different compositions.

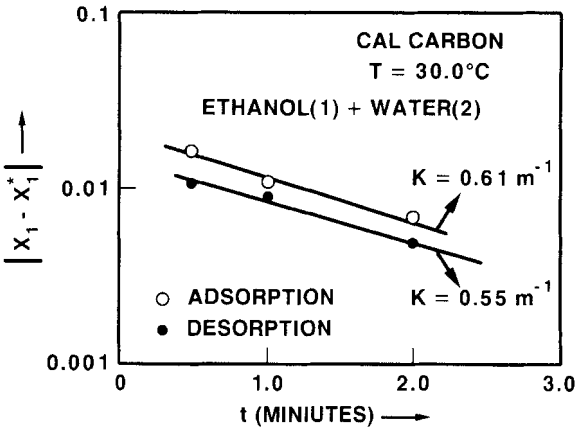

Figure 4. Examples of analysis of kinetic ad(de)sorption data from a differential test apparatus.

though ethanol-water mixture adsorption on carbon does not conform with the conditions used to derive Eq. 28. This, however, demonstrates the empirical usefulness of Eq. 28. The values of parameters m and S for the fit are 5.5 mol/kg and 42.0, respectively.

Column saturation capacities

We also measured the column saturation capacities ($\bar{n}^*$) at 25°C using the method described earlier at different compositions of ethanol. Figure 3 shows the results (circles). Large variation in $\bar{n}^*$ with x_1 is caused by large difference in the molar volumes of the adsorbates.

Ad(de)sorption kinetics

The differential test described earlier was used to measure the kinetics of ad(de)sorption for the ethanol-water mixtures on the CAL carbon. A closed-loop circulating apparatus was built in our laboratory for this purpose. Table 1 summarizes the conditions of the test runs for an adsorption and a desorption experiment, and Figure 4 shows the plots of transient changes in bulk-phase alcohol concentration with time according to Eq. 19. The mixing times for these experiments were about 0.25 min. The straight line plots of the data in Figure 4 indicate that the surface excess LDF model of kinetics for adsorption of liquid mixtures (Eq. 15) adequately describes the kinetics data for this system. The ad(de)sorption mass-transfer coefficients calculated from these plots are comparable, as shown in Table 1. In other words, no significant difference in mass-transfer resistances during these two processes was noticed.

We estimated the external-film mass-transfer resistances at the conditions of the test runs using a procedure described elsewhere (Rao et al., 1991) and found that more than 90% of resistances to ad(de)sorptive mass transfer were due to diffusional resistance of the adsorbates in liquid-filled macropores of the carbon.

Table 1. Summary of Differential Kinetic Test Results

	x_1^o	x_1^*	n^o, mol/kg	b, mol/kg	Re	k_1, s^{-1}
Adsorption	0.103	0.079	205	0	2.5	0.0100
Desorption	0.195	0.164	171	−3.2	3.5	0.0092

Column dynamics

We evaluated the dynamics of ad(de)sorption of ethanol-water mixture in a column packed with CAL carbon. The diameter of the column was 0.05 m and its length was 2.13 m. The experiments consisted of saturating the column with a pure liquid or a mixture of known composition and then displacing it with another pure liquid or mixture introduced into the column at a constant flow rate. The effluent column composition and quantity were measured as functions of time. A flow counter was used to measure the effluent quantity, and an automated gas chromatograph was used to measure the effluent liquid composition. Several thermocouples were imbedded in the column to measure temperature changes during the tests.

One adsorption experiment was conducted where a 20.9 mol % ethanol-water mixture was used to displace pure water from the column. Figure 5 shows the experimental (circles) effluent breakthrough curve (composition vs. time) for this experiment.

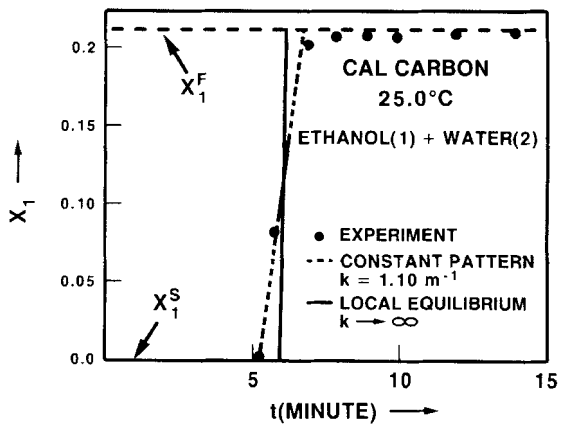

Figure 5. Column breakthrough curve for adsorption of 21.0 mol % ethanol-water mixture displacing pure water from a CAL carbon column.

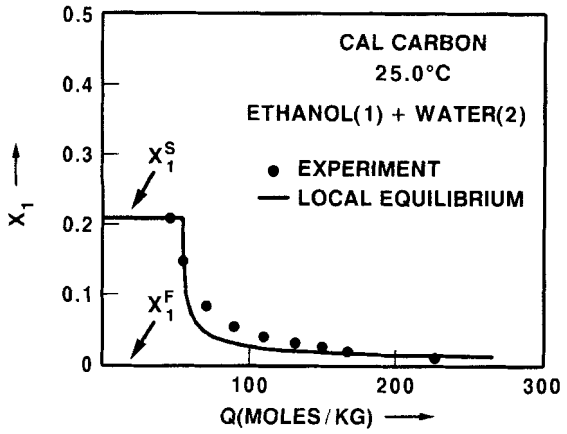

Figure 6. Column breakthrough curves for desorption of 21.0 mol % ethanol-water mixture by displacement with pure water in a CAL carbon column.

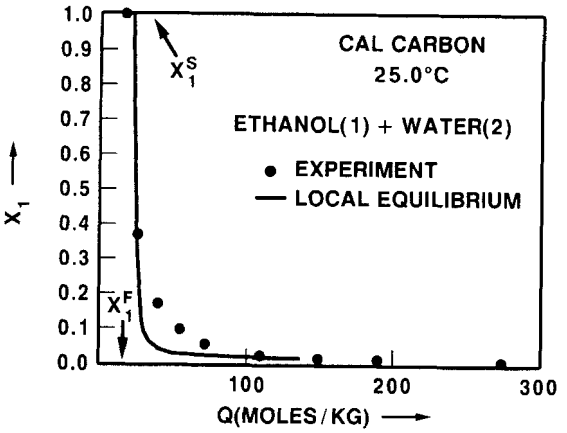

Figure 7. Column breakthrough curves for desorption of pure ethanol by displacement with pure water in a CAL carbon column.

A fairly sharp change in ethanol mole fraction (from 0 to 0.209) took place in a very short time, indicating that the mass-transfer zone length was short and the adsorption process was close to local equilibrium under the conditions of the test.

The constant pattern model for liquid-phase adsorption described earlier (Eq. 44) was used to describe the breakthrough curve of Figure 5 using the surface excess isotherm of Figure 2. The dashed line in Figure 5 shows the result. Figure 5 shows that a constant-pattern mass-transfer zone was formed for this system. The mass-transfer coefficient (k) obtained from this analysis was 0.018 s^{-1}, which compares very well with that (0.010 s^{-1}) obtained independently from the differential kinetic test (Table 1).

We also conducted two desorption tests where (a) the column saturated with 20.9 mol % ethanol-water mixture was displaced by pure water and (b) the column saturated with pure ethanol was displaced by pure water. Figures 6 and 7 show the experimental (circles) column effluent quantity against composition profiles for these tests. The breakthrough curves for these cases are diffused (elongated).

The local equilibrium model (Eqs. 25–27, 34–37) was used to describe the effluent profiles for the desorption runs using the isotherm of Figure 2. The solid lines in Figures 6 and 7 show that the local equilibrium model describes the desorption of alcohol from CAL carbon by displacement with water very well.

Table 2 summarizes the experimental and calculated values of Q^F and the first moments of the effluent breakthrough curves for the adsorption and desorption runs as well as those for the quantities E_1 and E_2 for the desorption runs. It also reports the experimental conditions for these runs. The agreements between the experiments and the model calculations are very good.

It may be concluded that ad(de)sorption of alcohol from water on the CAL carbon can be carried out very close to the local equilibrium conditions when the adsorbent particles are small and the models developed in this work based on surface excess as the primary variable to describe the extent of adsorption from liquid mixtures are adequate to describe the column dynamics.

The measurement of column temperatures during both adsorption and desorption runs of this study indicated that the columns were very nearly isothermal during these processes.

Conclusions

The isothermal kinetics and column dynamics for ad(de)sorption of bulk liquid mixtures can be fully described in terms of the pertinent surface-excess variables. The kinetics of ad(de)sorption can be formulated in terms of a surface excess linear-driving-force (SELDF) model under the framework of monolayer, pore-filling model of multicomponent liquid-phase adsorption. For a binary system, this model shows that the transient rate of change of surface excess of a component with time is equal to the product of a mass-transfer coefficient and the difference between the equilibrium surface excess at the transient bulk-phase composition and the actual transient surface excess of that component. For a multicom-

Table 2. Summary of Column Dynamic Test Results

	x_1^S	x_1^F	Q^F mol/m²·s	Q^S, mol/m²·s		E^A, mol/kg		E_1, mol/kg		E_2, mol/kg		$\hat{x}_1$	
				Calc.	Expt.	Calc.	Expt.	Calc.	Expt.	Calc.	Expt.	Calc.	Expt.
Adsorption													
Ethanol (1) + Water (2) displacing Water (2)	0.000	0.209	210	310	330	118	121	—	—	—	—	—	—
Desorption													
Water (2) displacing Ethanol (1) + Water (2)	0.209	0.000	310	200	210	66	76	55	54	111	114	0.027	0.041
Water (2) displacing Ethanol (1)	1.000	0.000	310	86	88	26	32	22	23	112	126	0.032	0.061

ponent system, the transient rate of change of surface excess of a component depends not only on the transient difference between the equilibrium and actual surface excesses of that component but also on such differences for other components present in the system. A differential kinetic test can be devised to measure the mass-transfer coefficients for ad(de)sorption from liquid mixtures using the SELDF model.

A local equilibrium model can be formulated to describe the column dynamics for ad(de)sorption of liquid mixtures using surface-excess variables. A self-sharpening or a proportionate-pattern mass-transfer zone can be formed depending on the characteristics of the surface-excess isotherms and the magnitude of dispersive forces in the column. A U-shaped surface-excess isotherm provides the driving force for a self-sharpening mass-transfer zone. The higher the selectivity of adsorption and the larger the ratio of pore volume capacity (m) to column saturation capacity ($\bar{n}^*$) of the adsorbates, the greater is the driving force for formation of self-sharpening mass-transfer zone.

An analytical relationship exists between the bulk liquid-phase composition and the surface excess inside the mass-transfer zone when a constant pattern mass-transfer zone is formed for a binary liquid system. In this case, the length of the mass-transfer zone (L_M) and the column-effluent composition-time profile can be calculated from the knowledge of the equilibrium surface-excess isotherm and the binary mass-transfer coefficient. L_M decreases when the selectivity of adsorption and the ratio ($m/\bar{n}^*$) increase.

On the other hand, the desorption of a more strongly adsorbed component by displacement with a less strongly adsorbed component is more efficient when the selectivity of adsorption for the first component is small. Desorption is also facilitated when ($m/\bar{n}^*$) is low.

Experimental kinetics and column dynamics data for adsorption of ethanol from water and desorption of ethanol by water on a large-pore activated carbon show that the kinetics can be adequately described by the SELDF model and these processes can be run close to local equilibrium conditions in a column when carbon particles are small in diameter.

Notation

b = slope of surface-excess isotherm
c = $[m/\bar{n}^*][1-m/\bar{n}^*]$
E^A = total specific stoichiometric effluent from column during adsorption
E_1 = total specific effluent from column having composition x_1^S during desorption
E_2 = total specific effluent from column with composition varying from x_1^S to x_1^F during desorption
E_2^1 = total specific amount of component 1 in E_2
F^A = total specific stoichiometric feed to column during adsorption
F^D = total specific feed to column during desorption
k = mass-transfer coefficient
L = column length
L_M = length of constant pattern mass-transfer zone
m = monolayer-pore-filling capacity of adsorbent
n = specific adsorption capacity
$\bar{n}$ = specific column saturation capacity (quantity in intra- and interparticle void space and the adsorbed phase)
n^e = surface excess
N = number of components
Q = molar flow rate per unit empty cross-sectional area of column
Re = particle Reynolds number at feed conditions
S = selectivity of adsorption of component 1 over component 2
t = time
x = bulk liquid-phase mole fraction
$\hat{x}$ = average concentration in E_2
z = distance in column from feed end

Greek letters

β = velocity
β = velocity for constant pattern zone
β_1 = m_3/m_1
β_2 = m_3/m_2
ρ_b = adsorbent bulk density
λ = $[n_1^{e*}(x_1^F) - n_1^{e*}(x_1^S)]/[x_1^F - x_1^S]$
θ = $(x_1 - x_1^S)/(x_1^F - x_1^S)$
θ^* = $[n_1^{e*}(x_1) - n_1^{e*}(x_1^S)]/[n_1^{e*}(x_1^F) - n_1^{e*}(x_1^S)]$
ϕ = value of θ defining bounds of constant-pattern mass-transfer zone

Superscripts

* = equilibrium condition
F = column feed condition
S = initial column saturation condition
o = total specific quantity in system

Subscript

i = component i

Literature Cited

Calgon Corporation Data Sheet, 23-105d (1983).

Chen, M. K. S., and S. Sircar, "Process for Preparing Alkyl Tert-Alkyl Ethers," U.S. Patent 5,030,768 (1991).

Gmehling, J., U. Onken, and W. Arit, "Vapor-Liquid Equilibrium Data Collection," DECHEMA, Frankfurt, Germany (1981).

Rao, M. B., S. Sircar, and T. C. Golden, "Equilibrium and Kinetics for Liquid Phase Adsorption of Bulk Acetic Acid from Water on Activated Carbon," Extended Abstract, Biennial Conference on Carbon, 54 (1991).

Sircar, S., "Process for Preparing Motor Fuel Grade Alcohol," U.S. Patent 5,030,775 (1991a).

Sircar, S., "Separation of Liquid Mixtures by Concentration Swing Adsorption," U.S. Patent 5,026,482 (1991b).

Sircar, S., "Thermodynamics of Adsorption from Binary Liquid Mixtures on Heterogeneous Solids," *J. Chem. Soc. Farad. Trans. I.*, **82**, 831 (1986).

Sircar, S., and R. Kumar, "Adiabatic Adsorption of Bulk Binary Gas Mixtures: Analysis by Constant Pattern Model," *Ind. Eng. Chem. Proc. Des. Dev.*, **22**, 271 (1983).

Sircar, S., A. L. Myers, and M. C. Molstad, "Adsorption of Dilute Solutes from Liquid Mixtures," *Trans. Farad. Soc.*, **66**, 2354 (1970).

Sircar, S., J. Novosad, and A. L. Myers, "Adsorption from Liquid Mixtures on Solids: Thermodynamics of Excess Properties and Their Temperature Coefficients," *Ind. Eng. Chem. Fundam.*, **11**, 249 (1972).

Yang, R. T., *Gas Separation by Adsorption Processes*, Butterworths, Boston (1987).

Manuscript received Nov. 19, 1991, and revision received Mar. 12, 1992. ◆